

# GAS DISCHARGE, PLASMA-BEAM DISCHARGE AND THEIR APPLICATIONS

<https://doi.org/10.46813/2023-146-121>

## TWO STAGE PLASMA SOURCE FOR LARGE SCALE BEAM GENERATION

*V.Yu. Bazhenov, A.M. Dobrovolskiy, V.V. Tsiolko, V.M. Piun  
Institute of Physics NAS of Ukraine, Kyiv, Ukraine  
E-mail: tsiolko@iop.kiev.ua*

The operation of a cylindrical plasma accelerator with an anode layer in the mode of ion space charge accumulation and the use of an ion flow accelerated by a space charge is investigated. In particular, the presence of high-voltage and diffusion modes with the formation of a secondary flow has been established. The output plasma flow current can reach 70% of the discharge current on the anode layer. The relationship between the connection scheme of the additional independent cathode and the plasma source parameters is shown.

PACS: 52.65.-y, 52.25.Xz, 52.27.Aj

### INTRODUCTION

Hall current plasma sources are popular among researchers due to their simple design and high reliability of plasma generation in a wide range of conditions. [1, 2] Sources of this type can have different designs, but all of them have the advantage of volumetric acceleration of ions from the ionization zone and the absence of output grids that should form an accelerated ion flow. [2] Among the sources with a closed current of electrons, the simplest by design are the sources with an anode layer (ALT). They can be useful both in outer space and in the technological processes of modifying the surface properties of materials or producing a modern element base of radio electronics [1 - 5]. These sources scale well for processing surfaces with large linear dimensions [6], but sometimes there is a need to process targets with a significant diameter. A typical accelerator with an anode layer is not suitable for such tasks. Previously, we created a source of a cylindrical plasma flow with its two-stage formation [7]. The peculiarity of the source is the ionization of the working gas in the anode layer on the periphery of the beam diameter, the accumulation of space charge in the main part of the volume of the beam formation and the formation of the beam itself by the space charge field. We also showed that there is a connection between the characteristics of the discharge with the anode layer and the characteristics of the cylindrical flow that is formed.

Such a source of ion-plasma flow can be well scaled to generate flows of different diameters and is interesting for further research and optimization.

In the paper, we investigate the characteristics of the source in conditions when the working gas is injected along the axis of flow formation. Such a scheme is not typical for sources with an anode layer and may not be optimal. However, this version of the gas feed automatically excludes the problem of the formation of two oppositely directed plasma flows from the volume of the device. Also, such gas feed simplifies the design of the plasma source.

### 1. EXPERIMENTAL DEVICE AND DIAGNOSTICS

The experimental device was placed inside a cylindrical vacuum chamber with a diameter of 500, a length of 700 mm and a volume of 140 l. The chamber was galvanically connected to the ground. The chamber also contained:

- holders made of insulating material (poly-methyl methacrylate), the design of which made it possible to move the device along the chamber, as well as to center it at the chamber axis;

- computer-controlled moveable table (minimum step size along the chamber is 1 mm) for placement of diagnostic devices required in the investigations (magnetic and Langmuir probes, collectors, optical elements, etc.).

The chamber was evacuated through a diaphragm with a regulated opening by a steam-oil pump with a speed of 2500 l/s. Minimum residual pressure in the chamber was about  $8 \cdot 10^{-6}$  Torr. For the regulated supply of argon into the device, gas feeder SNA-2 was used. Gas pressure inside the chamber was measured by means of vacuum gauge VIT-2.

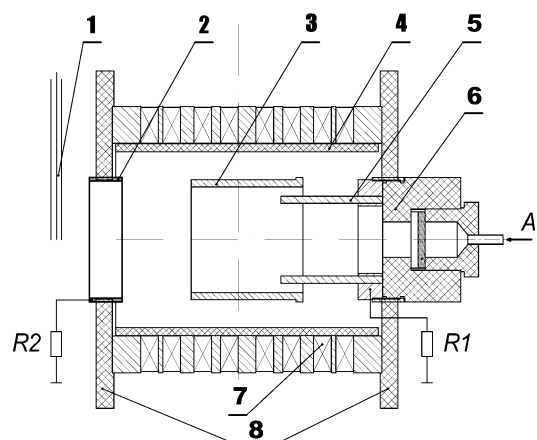


*Fig. 1. Scheme of experimental device: 1 – probe; 2 – “external” cathode; 3 – anode; 4 – cylinder; 5 – “internal” cathode; 6 – gas feed system; 7 – magnetic system; 8 – dielectric flanges*

Anode 3 of the device with an internal diameter of 67 mm and a length of 55 mm was located in the middle of a quartz cylinder 4 with an internal diameter of 95 mm and a length of 150 mm (Fig. 1). The “inner” cathode 1 consisted of 6 rods with a diameter of 3 mm arranged in a circle at a certain distance from the inner surface of the anode. The role of the “external” cathode 2 was performed by a metal ring with an inner diameter of 65 mm and a height of 20 mm. Both cathodes were mounted on dielectric flanges 8. Argon was fed into the middle of the device through a system 6 with grids for laminarization of the gas flow. The argon pressure in the chamber varied within  $(0.4...6) \cdot 10^{-4}$  Torr (according to estimates, the argon pressure in the device cavity was approximately 1.5...2 times higher). The magnetic system 7 on permanent magnets created a magnetic field in the gap between the cathodes 1 and the anode with a magnitude of 650...700 Oe.

When conducting experimental studies, the pulse-periodic mode of operation of the power source was used in order to prevent overheating of the elements of both the source itself and the discharge system. This mode was provided by cutting 1, 2 or 4 consecutive voltage oscillations of the standard (50 Hz frequency) power net, which were repeated with a period of 0.5, 1 or 2 s. The mode with 4 oscillations and a repetition period of 2 s was most often used in the experiments. The maximum amplitude of voltage pulse was 4.5 kV, and the maximum current was up to 1 A.

When studying the properties of the device, the amplitude values of the voltages and currents of the cathodes 1, 2 ( $U_{c1}$ ,  $U_{c2}$ ,  $I_{c1}$ ,  $I_{c2}$ , respectively), anode voltage  $U_a$ , total anode current  $I_{sum}$  and the current  $I$  outcoming from the device to the chamber were measured for different argon pressure values and resistances  $R1$ ,  $R2$ . As well, floating potential amplitudes  $U_f$  in the plasma outside the discharge volume were measured by means of Langmuir probe 8 located near the cathode 2.

## 2. EXPERIMENTAL RESULTS

During the research, the pulsed voltage from the power source was applied to the discharge anode relatively to the grounded chamber. It was established that with the described configuration of the electrodes of the device, the discharge was ignited only when the cathode 2 was connected to the chamber via a resistance of approximately 100 k $\Omega$  or less. Also, during the research, cathode 1 was connected to the grounded chamber through resistance  $R2$  of different magnitudes. This made it possible to “raise” the potentials of the cathodes during the discharge glow to simulate the operation of the device in free space. The study of the characteristics of the device was carried out using resistances  $R1$ ,  $R2$  with a value from several hundreds of ohms to tens of kilohms. This article presents the results of researches performed using  $R1$ ,  $R2$  with values of 820  $\Omega$  and 10 k $\Omega$  in various combinations of their connection to cathodes 1 and 2.

The discharge was ignited at a pressure of  $\approx 4 \cdot 10^{-5}$  Torr and existed in two modes – low-current and high-current. Typical current-voltage  $U_a$ - $I_d$  characteristics (CVC) of the discharge in these two modes are presented in Fig. 2. (When discussing the processes that

take place in the device, it should always be borne in mind that in reality the discharge voltage, i.e. the potential difference between the anode and the cathode can be much lower than the voltage at the anode). In the low-current regime, which existed only at pressures less than  $P_{thr} \approx (6...7) \cdot 10^{-5}$  Torr, the maximum discharge current  $I_d$  (that is, the current through both cathodes  $I_{c1}+I_{c2}$ ) did not exceed a few milliamperes at the maximum anode voltage  $U_a$  about 4 kV. In this mode, the glow of the discharge was observed mainly in the gap between the cathode rod 1 and the anode and on the axis of the system. The current-voltage characteristic of this discharge was weakly dependent on the combination of resistance values in the circuits connecting the cathodes to the grounded chamber.

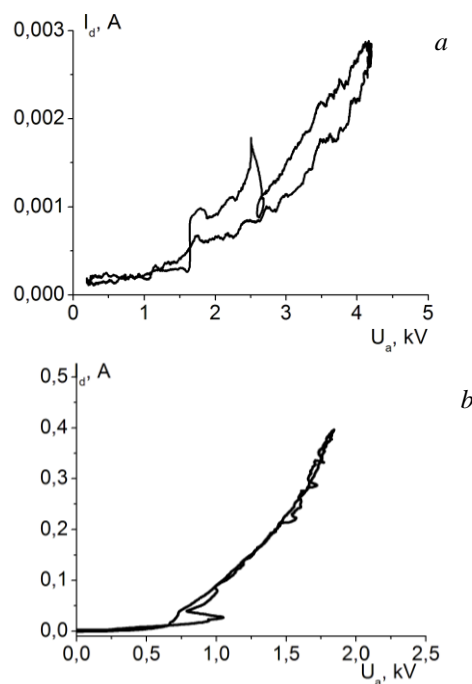


Fig. 2. Typical current-voltage characteristics of the discharge in different glow modes:  $5 \cdot 10^{-5}$  Torr (a);  $3.6 \cdot 10^{-4}$  Torr (b).  $R1 = 820 \Omega$ ,  $R2 = 10 \text{ k}\Omega$

When the threshold pressure  $P_{thr}$  is exceeded, the discharge switches to high-current mode – in the range of pressures up to  $\approx 1 \cdot 10^{-5}$  Torr, the discharge current  $I_d$  increases sharply from a few milliamperes to  $\approx (100...200)$  mA. At further pressure increase the discharge current growth rate decreases. In general, all measured dependencies  $I_d$ ,  $U_d$ ,  $I$ ,  $U_{c1}$ ,  $U_{c2}$ ,  $I_{c1}$ ,  $I_{c2}$  on argon pressure were to a greater or lesser extent a function of the values of the resistances  $R1$ ,  $R2$ . Some peculiarities of the influence of the values of these resistances on the dependence of the measured values on argon pressure will be discussed in more detail below.

An increase in argon pressure also leads to a change in the spatial distribution and brightness of the discharge plasma glow. As the pressure increases, both the dimensions (diameter and length) and the brightness of the glow on the axis of the system increase. The color of the plasma glow also changes. At a pressure of  $\approx 5 \cdot 10^{-4}$  Torr, the exit of this spindle-shaped glow beyond the plane of the dielectric flange with the cathode 2 is observed.

An example of the glow nature of the discharge plasma in the high-current mode is presented in Fig. 3 (a Langmuir probe for measuring the floating potential is visible in the foreground). As can be seen from Fig. 3,a, the brightness of the glow of the central part significantly exceeds the brightness of the glow of the surrounding space. This indicates that in this regime the processes of ionization and excitation of argon atoms mainly occur on the axis of the system.

The bright ring-like glow near the surface of the quartz cylinder is associated with the presence of two cusps (zero strength regions) in the magnetic field of the device [8] (these cusps are at a distance of 15 mm from the inner surface of the dielectric flanges). The presence of these cusps leads to the exit of magnetized electrons to the surface of the quartz cylinder and the formation of virtual cathodes during the discharge glow in the high-current mode. It should be noted that a separate article will be devoted to a more detailed study of the role and influence on the discharge parameters of these virtual electrodes. And now we only note that the formation of these virtual cathodes plays a significant role in the generation of plasma flows that are injected outside the device.

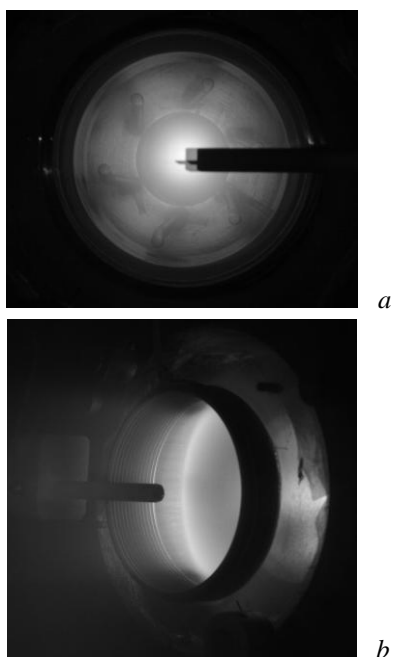


Fig. 3. Photos of the discharge plasma glow at argon pressure  $3.5 \cdot 10^{-4}$  Torr viewed at different positions: from the end (a); at an angle of  $\approx 45^\circ$  to the system axis (b)

Let us consider how different combinations of resistance values  $R_1$ ,  $R_2$  affect the values and dependence of the amplitudes of the discharge device parameters on the argon pressure. As can be seen from Fig. 4, regardless of which cathodes are connected to the resistors of  $820 \Omega$  and  $10 \text{ k}\Omega$ , voltages  $U_a$ ,  $U_f$  in both cases show practically the same behavior and the value. In both cases, with increasing pressure,  $U_a$  monotonically drops from  $\approx 4$  to  $\approx 1.7 \text{ kV}$  (with a bend near  $\approx 1 \cdot 10^{-4}$  Torr), and  $U_f$  first increases sharply, reaching a value of  $\approx (1.6 \dots 1.7) \text{ kV}$  at a pressure of  $\approx 1 \cdot 10^{-4}$  Torr, and then (synchronously with  $U_a$ ) decreases to  $\approx 1.2 \text{ kV}$ . The

initial increase in  $U_f$  is due to the fact that the plasma density near the probe (that is, outside the device) increases simultaneously with the pressure. As a result, the potential of the floating probe begins to be "linked" to the potential of the anode  $U_a$ . And starting from a certain pressure, the potential of the probe changes synchronously with the change in  $U_a$ .

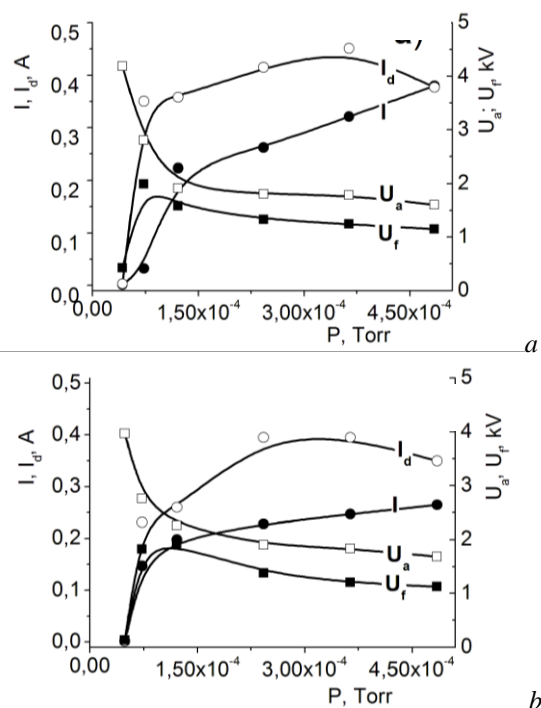


Fig. 4. Dependencies of amplitude values of the discharge parameters  $I_\omega$ ,  $I$ ,  $U_\omega$ ,  $U_f$  on argon pressure:  $R_1 = 820 \Omega$ ,  $R_2 = 10 \text{ k}\Omega$  (a);  $R_1 = 10 \text{ k}\Omega$ ,  $R_2 = 820 \Omega$  (b)

At pressure  $\approx (1 \dots 1.5) \cdot 10^{-4}$  Torr in both cases, changes also occur in the behavior of  $I_d$  and  $I$  – their growth rates decrease with pressure. Whereas in subsequent the linear nature of the growth of the outgoing current  $I$  is preserved, then the discharge current  $I_d$  at pressures greater than  $\approx 3.5 \cdot 10^{-4}$  Torr begins to decrease. The decrease in  $I_d$  and the simultaneous increase in  $I$  compensate for each other, so that the full anode current  $I_{\text{sum}}$  remains at the same level.

The probable reason for such an effect may be the following. The increase in the value of  $I$  with increasing pressure means that the plasma from the device spreads further and at a certain moment collides with the grounded walls of the chamber. The density, as well as the potential of this plasma, can be high enough to create a sufficiently strong electron current from the walls of the chamber due to ion-electron emission. Since in the pressure range  $\approx (3 \dots 5) \cdot 10^{-4}$  Torr the value of the anode voltage  $U_a$  changes weakly with pressure, then to maintain the value of  $I_{\text{sum}}$  at a certain level in the presence of current from the walls, the need for current from cathodes 1, 2 decreases.

It should be noted that starting from such a critical pressure  $P_{cr}$ , when the further increase in pressure is accompanied by an increase in the value of  $I$  with a simultaneous decrease of the current  $I_d$ , the plasma flow coming outside the device cannot be considered free. In

other words, at such pressures, it is necessary to take into account the effect of charged particles emitted from the surface of the chamber on the operation of the device itself.

In general, as can be seen from Fig. 4, in both cases the outgoing current  $I$  is about 70% of the discharge current  $I_d$ , but in the case of the option of connecting  $R1 = 820 \Omega$ ,  $R2 = 10 \text{ k}\Omega$ , it is possible to obtain about 30% more outgoing current.

As already noted above, the discharge voltage, that is, the potential difference between the anode and the cathode (cathodes), can be much smaller than the anode voltage  $U_a$ . This is clearly visible from Fig. 5, b, which shows the dependences of the amplitude values of the potentials of the anode and both cathodes on the argon pressure at the same values of  $R1$ ,  $R2 = 10 \text{ k}\Omega$ . It can be seen that despite the identical values of  $R1$  and  $R2$ , the potentials of the cathodes  $U_{c1}$  and  $U_{c2}$  are not significantly different.

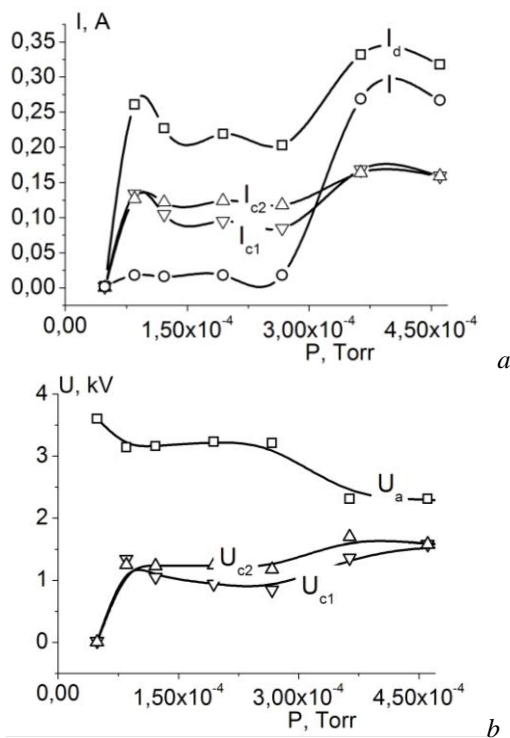


Fig. 5. Dependencies of amplitude values of the discharge parameters:  $I_d$ ,  $I$ ,  $I_{c1}$ ,  $I_{c2}$  (a);  $U_a$ ,  $U_{c1}$ ,  $U_{c2}$  on argon pressure (b).  $R1 = 10 \text{ k}\Omega$ ,  $R2 = 10 \text{ k}\Omega$

Comparison of Figs. 4, a, and 5, a shows that the application of a symmetrical cathodic load significantly affects the behavior of the device parameters. Thus, in contrast to the asymmetric loading of cathodes, with symmetrical loading, the plasma flow to the outside of the device is practically absent up to a pressure of  $\approx 3 \cdot 10^{-4}$  Torr. When the pressure increases above this threshold, the outgoing current  $I$  increases sharply, reaching about 80% of the discharge current at  $4 \cdot 10^{-4}$  Torr. With a further increase in pressure, magnitude of the current  $I$  decreases rapidly.

In the case of symmetrical connection of resistances  $R1$ ,  $R2$ , the maximum value of the outgoing current both in relation to the discharge current and in absolute value are generally close to the values of  $I$  in the case of asymmetrical connection.

## SUMMARY

The performed study shows the possibility of forming a large-diameter plasma flow in a source with separation of ionization zones and flow formation due to the accumulated space charge. The output current can reach up to 70% of the discharge current and depends on the discharge conditions. The obtained results also show the dependence of the flow formation on the potentials of the cathodes, which are electrically independent. This demonstrates the possibility of independent control of the energy of the ions in the flow regarding to the potential in the discharge with the anode layer.

The working gas supply scheme used is not optimal from the viewpoint of gas efficiency. However, this issue is not a key in technological applications. At the same time, this scheme simplifies the design and operation of the source. The issue of effective control of the ion energy in the flow regardless of the main discharge voltage remains unsolved. The outlined problems will be the subject of further research, as well as the operation of the source in the mode with the working gas feed through the anode.

The work is supported by grant 1.4. B/215 of the National Academy of Sciences of Ukraine.

## REFERENCES

1. I. Levchenko, S. Xu, S. Mazouffre, F. Taccogna, and K. Bazaka, Perspectives, frontiers, and new horizons for plasma-based space electric propulsion // *Phys. Plasmas* 27. 2020, p. 020601; doi: 10.1063/1.5109141.
2. K. Holste, P. Dietz, S. Scharmann, et al. Ion thrusters for electric propulsion: Scientific issues developing a niche technology into a game changer // *Rev. Sci. Instrum.* 91. 2020, p. 061101; doi: 10.1063/5.0010134.
3. Yaroshchuk, R. Kravchuk, A. Dobrovolskyi, L. Qiu, O.D. Lavrentovich. Planar and tilted uniform alignment of liquid crystals by plasma-treated substrates // *Liquid Crystals*. 2004, v. 31, № 6, p. 859-869; doi: 10.1080/02678290410001703145.
4. A.N. Dobrovols'kii, A.A. Goncharov, S.N. Pavlov, O.A. Panchenko, I.M. Protsenko. Modernized technological accelerator with anode layer for ion cleaning // *Problems of Atomic Science and Technology*. 2002, № 4, p. 176-178.
5. O.I. Girka, K.I. Lee, Y.S. Choi, S.O. Jang. Ion beam figuring with focused anode layer thruster // *Rev Sci Instrum* 93. 2022, p. 063304; doi: 10.1063/5.0071800.
6. A.A. Goncharov, A.M. Dobrovolskii, S.N. Pavlov, O.A. Panchenko, I.M. Protsenko. Technological accelerator with closed electron drift for surface treatment // *Problems of Atomic Science and Technology*. 2000, № 6, p. 160-162.
7. I. Litovko, A. Goncharov, A. Dobrovolskyi, and I. Naiko. The Emerging Field Trends Erosion-Free Electric Hall Thrusters Systems // *Plasma Science and Technology* / Edited by Aamir Shahzad, InTechOpen, London, 2022. Chapter 11, p. 195-214 DOI: 10.5772/intechopen.99096.
8. A.M. Dobrovols'kii, A.N. Evsyukov, A.A. Goncharov, I.M. Protsenko. Cylindrical magnetron based on the plasmaoptical principles // *Problems of Atomic Science and Technology. Series "Plasma Physics"*. 2007, № 1, p. 151-153.

Article received 15.06.2023

## **ДВОСТУПЕНЕВЕ ДЖЕРЕЛО ПЛАЗМИ ДЛЯ ГЕНЕРУВАННЯ ШИРОКОМАШТАБНОГО ПРОМЕНЯ**

***В.Ю. Баженов, А.М. Добровольський, В.В. Цюлко, В.М. Піун***

Досліджено роботу циліндричного плазмового прискорювача з анодним шаром у режимі накопичення об'ємного заряду іонів та використання потоку іонів, прискореного об'ємним зарядом. Зокрема, встановлено наявність високовольтного та дифузійного режимів з утворенням вторинного потоку. Струм вихідного плазмового потоку може сягати 70% розрядного струму на анодному шарі. Показано зв'язок між схемою підключення додаткового незалежного катода та параметрами плазмового джерела.